

# A Chemically Induced Vaccine Strategy for Prostate Cancer

Anna Dubrovskaya,<sup>†,‡</sup> Chanhyuk Kim,<sup>†,‡</sup> Jimmy Elliott,<sup>‡</sup> Weijun Shen,<sup>‡</sup> Tun-Hsun Kuo,<sup>†</sup> Dong-In Koo,<sup>†</sup> Chun Li,<sup>‡</sup> Tove Tuntland,<sup>‡</sup> Jonathan Chang,<sup>‡</sup> Todd Groessl,<sup>‡</sup> Xu Wu,<sup>‡</sup> Vanessa Gorney,<sup>‡</sup> Teresa Ramirez-Montagut,<sup>‡</sup> David A. Spiegel,<sup>§</sup> Charles Y. Cho,<sup>‡,\*</sup> and Peter G. Schultz<sup>†,\*</sup>

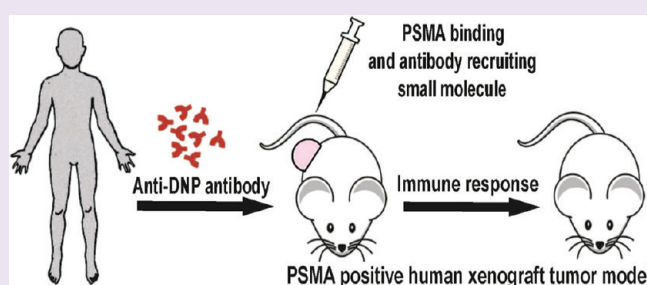
<sup>†</sup>Department of Chemistry, The Scripps Research Institute, 10550 North Torrey Pines Road, La Jolla, California 92037, United States

<sup>‡</sup>Genomics Institute of the Novartis Research Foundation, 10675 John Jay Hopkins Drive, San Diego, California 92121, United States

<sup>§</sup>Department of Chemistry, Yale University, 225 Prospect Street, New Haven, Connecticut 06520, United States

## Supporting Information

**ABSTRACT:** Here we report the design and evaluation of a bifunctional, small molecule switch that induces a targeted immune response against tumors *in vivo*. A high affinity ligand for prostate specific membrane antigen (PSMA) was conjugated to a hapten that binds dinitrophenyl (DNP)-specific antibodies. When introduced into hu-PBL-NOD/SCID mice previously immunized with a KLH-DNP immunogen, this conjugate induced a targeted antibody-dependent cellular cytotoxicity (ADCC) response to PSMA-expressing tumor cells in a mouse xenograft model. The ability to create a small molecule inducible antibody response against self-antigens using endogenous non-autoreactive antibodies may provide advantages over the autologous immune response generated by conventional vaccines in certain therapeutic settings.



Prostate cancer is the second most common cause of cancer death in men. Despite improvements in local treatment, 20–40% of men with apparently localized disease develop invasive and drug-resistant metastatic cancers upon relapse. Vaccine therapy is an attractive approach to prostate cancer treatment because of the presence of highly expressed tumor-associated antigens such as prostate specific antigen (PSA), prostate acid phosphatase (PAP), and prostate specific membrane antigen (PSMA). Clinical trials of immunotherapy-based prostate cancer therapies include vaccination with recombinant protein or DNA, cell-based strategies, and antibodies conjugated to drugs or radiolabels.<sup>1</sup> Although Sipuleucel-T has demonstrated modest survival benefit, other anticancer vaccine strategies have failed in clinical trials due to tumor-induced immune dysfunction<sup>2–4</sup> and severe side effects.<sup>5</sup>

The development of therapeutic vaccines against self-proteins is complicated by the relatively long lifetime of the resulting antibodies in serum, which may lead to a lasting autoimmune response. One possible solution to this problem is to control the temporal presentation of an antigen so that the immune response to self can be terminated when desired. This can be accomplished by the use of a bifunctional small molecule that selectively binds a target self-protein with high affinity and presents a hapten that binds circulating antibodies (ligand-mediated immunogenicity).<sup>6–8</sup> The latter can be generated *a priori* by immunization with a non-self antigen. Antibodies bound to the self-protein through the small adaptor molecule then kill the target cells through antibody-dependent cytotoxicity (ADCC) and complement-dependent

cytotoxicity (CDC). Here we test the feasibility of this approach in an *in vivo* prostate cancer xenograft model.

## RESULTS AND DISCUSSION

The design of our drug-inducible vaccine is based on the bifunctional molecule **1**, which consists of a PSMA-specific ligand linked to a highly immunogenic 2,4-dinitrophenyl (DNP) group (Figure 1). PSMA expression increases with disease progression and is highest in metastatic, hormone-refractory prostate cancers, thus making it an attractive target.<sup>9</sup> PSMA is also present in the neovasculature of other solid tumors (*e.g.*, pancreatic ductal carcinoma, colon adenocarcinoma, glioblastoma multiforme, and non-small cell lung carcinoma) making anti-PSMA therapies potentially applicable to a variety of neoplasms.<sup>9</sup> To target PSMA with high affinity and selectivity, ligand **1** contains a 2-[3-(1,3-dicarboxypropyl)-ureido]pentanedioic acid (DUPA) moiety, a PSMA-specific ligand reported by Kozikowski and Low,<sup>10,11</sup> coupled to DNP through a hydrophilic polyethylene glycol linker (ligand **1**, Figure 1b). We confirmed that the combination of an anti-DNP antibody, ligand **1**, and soluble PSMA forms a ternary complex with an *in vitro* binding assay (Supplementary Figure S1a). We further showed that ligand **1** recruits an anti-DNP antibody to the surface of PSMA-expressing LNCaP cells with an EC<sub>50</sub> of 2.48 nM (Supplementary Figure S1b and S1c). These results are in agreement with an earlier study by Spiegel

Received: July 1, 2011

Accepted: August 26, 2011

Published: September 21, 2011

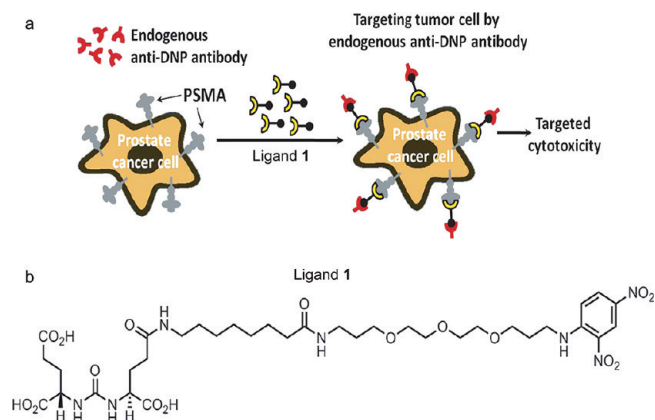


**Figure 1.** Chemically induced anticancer immunity using a PSMA-targeting, antibody-recruiting small molecule (ligand 1). (a) Schematic representation of the approach to prostate cancer targeting *in vivo* by chemically induced immune recognition. (b) Structure of ligand 1.

and co-workers that showed that a PSMA-specific DNP conjugate can induce formation of an anti-DNP antibody–compound–enzyme complex and induce cell-mediated cytotoxicity against prostate cancer cells *in vitro*.<sup>12</sup>

To test whether ligand 1 can induce antitumor immunity to human PSMA-expressing tumor cells *in vivo* requires an animal model with a humanized immune response. One such model involves engraftment of immunocompetent human peripheral blood lymphocytes (HuPBL) into SCID mice.<sup>13</sup> Human PBLs were obtained from a normal donor, purified, and injected intraperitoneally (ip) into NOD/SCID mice ( $20 \times 10^6$  cells per mouse). Six weeks after HuPBL injection, spleen tissues from hu-PBL-NOD/SCID mice and mice that were not engrafted with human lymphocytes were analyzed for the presence of CD3+, CD8+, and CD4+ human lymphocytes. Flow cytometry analysis and immunostaining confirmed repopulation with human lymphocytes (Supplementary Figure S2).

Because ligand 1 contains a dinitrophenyl group that binds to anti-DNP antibodies with high affinity, it may be possible to use endogenous anti-DNP antibodies to target PSMA-positive prostate tumors and elicit an antitumor response. Anti-DNP antibodies are present in normal human serum<sup>14</sup> and are competent to mediate targeted cytotoxicity<sup>15</sup> (Supplementary Figure S3). Notably, we observed a detectable level (a titer of 1:1000) of anti-DNP antibodies in hu-PBL-NOD/SCID even prior to vaccination, suggesting that human B cells can produce endogenous anti-DNP antibodies after HuPBL engraftment without additional immunization (Supplementary Figure S3). However, to elevate the level of human anti-DNP antibodies in the bloodstream of the mice, we immunized hu-PBL-NOD/SCID mice with DNP coupled to keyhole limpet hemocyanin (KLH) and analyzed the serum level of DNP-specific human IgG by ELISA (Supplementary Figure S4). After two immunizations of hu-PBL-NOD/SCID mice with 100  $\mu$ g of DNP-KLH in PBS emulsified with complete and then incomplete Freund's Adjuvant, we observed an elevated titer of anti-DNP antibody (1:100,000) in mouse serum.

We next confirmed that antibodies in serum from DNP-KLH vaccinated mice can bind PSMA-expressing prostate cancer cells *in vitro* in the presence of ligand 1. We performed live-cell flow cytometry assays with PSMA-expressing prostate LNCaP cells and PSMA-negative prostate DU145 cells with serum from

hu-PBL-NOD/SCID mice. These experiments showed specific binding of anti-DNP antibodies to LNCaP cells in the presence of 62 nM of ligand 1 that could be competed with free DUPA (Figure 2a); no binding was observed to PSMA-negative DU145 cells. The flow cytometry data was confirmed by immunofluorescence microscopy; no fluorescence was observed in the presence of control serum from hu-PBL-NOD/SCID mice that were not vaccinated with DNP-KLH (Figure 2b). Ligand 1 was then tested for its ability to kill prostate cancer cells through an ADCC mechanism through interaction of Fc receptors on cytotoxic effector cells with the Fc portion of antibodies bound to the surface of target cells.<sup>16</sup> A 2.4- to 6.0-fold increase in killing of LNCaP cells compared to that with DUPA-treated LNCaP cells or DU145 cells was detected with various dilutions of mouse anti-DNP serum in the presence of 62 nM ligand 1. In contrast, no differences in cell-mediated toxicity were observed under identical conditions using PSMA-negative DU145 prostate cancer cells, with or without competing DUPA ligand (Figure 2c).

We next tested the ability of ligand 1 to induce a robust antitumor immune response (scheme outlined in Supplementary Figure S5). Two weeks after injection of peripheral blood mononuclear cells (PBMC) into NOD/SCID mice, mice were immunized with DNP-KLH and boosted 2 weeks later. Three days after the first immunization,  $5 \times 10^5$  LNCaP cells or  $5 \times 10^4$  DU145 cells were injected subcutaneously (sc), and xenograft human tumors grew to a volume of 50–70 mm<sup>3</sup> after 2 weeks. Mice were treated with DUPA (4 mg/kg, intravenously (iv)) or ligand 1 (4 mg/kg, iv) three times per week for 2 weeks (ligand 1 has a  $t_{1/2}$  of 1.5 h and AUC of  $1.6 \text{ h} \cdot \mu\text{M}$  in mice (Supplementary Figure S6)). Treatment with ligand 1 inhibited the growth of PSMA-positive LNCaP tumors 4.8-fold relative to the control groups treated with DUPA (Figure 3). In contrast, PSMA-negative DU145 tumors were not susceptible to ligand 1-mediated tumor inhibition, and no significant differences in tumor growth were observed in the treated animal groups (Figure 3). Tumors grown in nonhumanized NOD/SCID mice and treated with ligand 1 (4 mg/kg, iv) were used as the controls and showed no significant differences in tumor growth relative to PBS-treated mice.

Delivery of anti-DNP antibody to cancer cells by ligand 1 should convert poorly immunogenic tumors into highly immunogenic targets and make them susceptible to ADCC.<sup>17,18</sup> To further investigate the mechanisms underlying the antitumor effects of this ligand-inducible vaccine, we analyzed markers for immune cell-mediated tumor cell killing in the tumor microenvironment using immunohistochemical analysis. Cytotoxic lymphocytes act through delivery into target cells of cytotoxic enzymes, such as granzyme B, that promote apoptosis through activation of caspases 3, 7, 8, and 1 and through mitochondrial disruption.<sup>19</sup> Immunostaining of the xenograft tumors with anti-granzyme B antibody revealed a significant accumulation of enzyme in LNCaP tumors exposed to ligand 1 as compared to DUPA-treated LNCaP tumors (Figure 4a). In contrast, PSMA-negative DU145 prostate tumors showed a low level of granzyme B expression (Supplementary Figure S7a). To test whether accumulation of cytotoxic cells is associated with enhancement of antitumor cytotoxicity, tumors from experimental animals were analyzed by TUNEL assay and stained with anti-activated caspase-3 antibody. As depicted in Figure 4b and Supplementary Figure S7b–d, a greater than 3-fold increase in the number of apoptotic cells was observed in LNCaP tumors exposed to

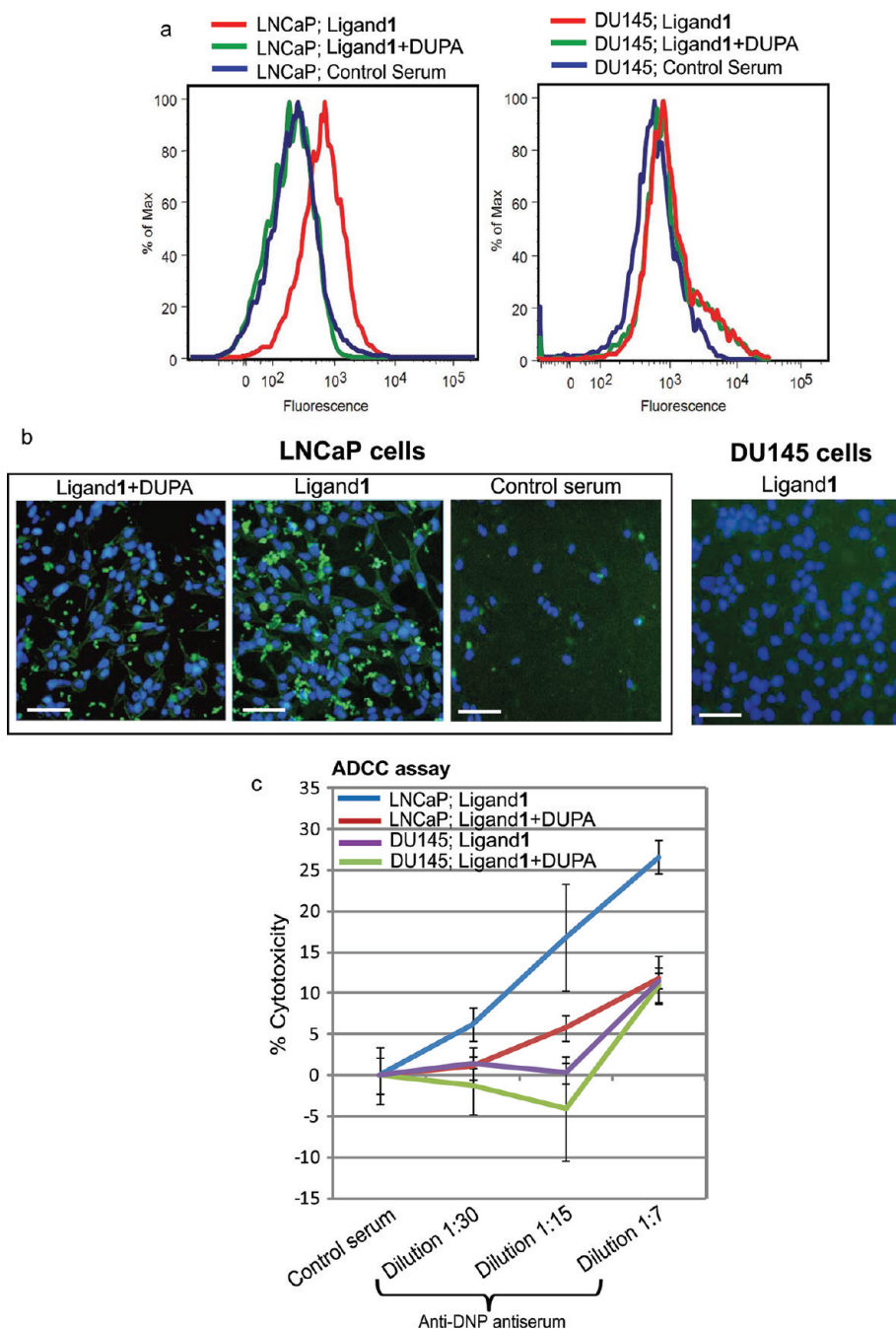


**Figure 2.** Ternary complex formation and ADCC with anti-DNP serum, ligand 1, and prostate cancer cells *in vitro*. (a) Representative flow cytometry histograms showing specific binding of anti-DNP antiserum to LNCaP cells in the presence of ligand 1. Anti-DNP serum was generated in hu-PBL-NOD/SCID mice immunized with DNP-KLH and used at 1:5 dilution 4 weeks after first immunization. Cell suspensions were incubated with DUPA (100 nM) or PBS followed by ligand 1 (62 nM), anti-DNP serum and APC-conjugated goat antihuman IgG. No appreciable ternary complex formation was observed using PSMA-negative DU145 cells. (b) Fluorescence microscopy illustrating specificity of anti-DNP serum from hu-PBL-NOD/SCID mice immunized with DNP-KLH to LNCaP cells coated by ligand 1. Ligand 1 (62 nM) or DUPA (100 nM) plus 62 nM ligand 1 (competition experiment) were added to cells followed by mouse anti-DNP serum at 1:11 dilution and R-PE conjugated goat antihuman Ig antibody. For negative control experiments, control serum from nonimmunized hu-PBL-NOD/SCID mice was added. Nuclear staining (4',6-diamidino-2-phenylindole) is shown in blue, and DNP staining is shown in green. Scale bars indicate 100  $\mu\text{m}$ . (c) Antibody-dependent cellular cytotoxicity assays. Ligand 1 (62 nM) or ligand 1 (62 nM) + DUPA (100 nM) and anti-DNP serum at the indicated dilutions were added to cells followed by addition of human PBMCs. The percent cytotoxicity was assessed using Calcein-AM to determine cell viability. The enhanced killing of PSMA-positive LNCaP cells was detected with antibody concentrations comparable to those in the human bloodstream. In contrast, cell-mediated toxicity was significantly lower under identical conditions with the PSMA-negative DU145 prostate cancer cells or upon addition of competing DUPA. Error bars represent SEM.

ligand 1 as compared to DUPA-treated LNCaP tumors. DU145 tumors were less susceptible to drug-mediated cytotoxicity, and

a low percentage of apoptotic cells (<0.5%) was observed in tumors treated with either DUPA or ligand 1.

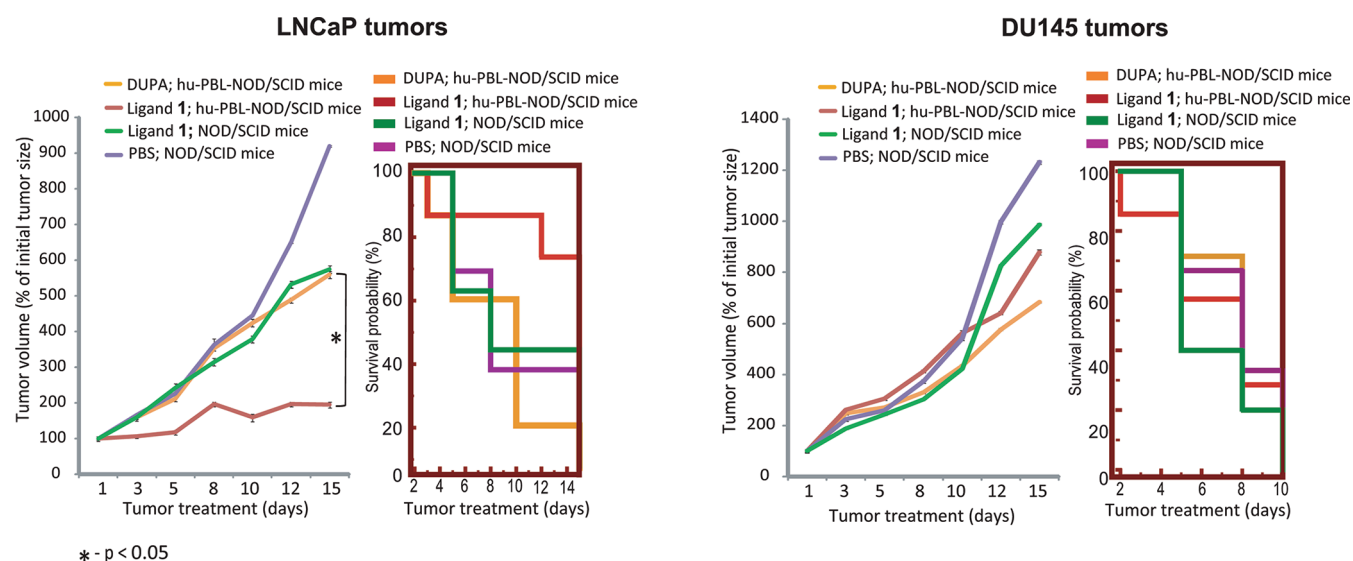


**Figure 3.** Efficacy of ligand 1 in a prostate cancer xenograft model. Hu-PBL-NOD/SCID mice bearing xenograft human tumors were treated with DUPA in PBS (4 mg/kg, iv) or ligand 1 in PBS (4 mg/kg, iv) three times per week for 2 weeks. Treatment with ligand 1 inhibited the growth of PSMA-positive tumors 4.8-fold relative to the control groups treated with DUPA. In contrast, PSMA-negative tumors were not susceptible to ligand 1-mediated cell killing, and no significant differences in tumor growth were observed in the treated animal groups. Tumors grown in nonhumanized NOD/SCID mice and treated with ligand 1 (4 mg/kg, iv) or PBS were used as the controls. Each experimental group contained at least five mice. Error bars represent SEM.

Vaccine-induced cytotoxic responses can be mediated by a number of different cell types, including NK cells and cytotoxic T cells. Tumor sections from LNCaP and DU145 xenografts from animals in Figure 3 were stained for the NK-specific marker CD56. A significantly greater number of infiltrating CD56+ and CD16+ NK cells in ligand 1-treated LNCaP tumors was observed as compared to DUPA-treated LNCaP (a greater than 7-fold increase) and DU145 tumors (Figure 4c and d and Supplementary Figure S7e and f). The presence of NK cells in the tumors would be consistent with ADCC as a mechanism for ligand 1-mediated reduction in tumor growth. Since other mechanisms may also contribute to antitumor activity, we stained tumor sections for other markers. CD3 is a marker for T cell populations including helper T cells and killer T cells.<sup>20</sup> As shown in Figure 4e and Supplementary Figure S7g, ligand 1-treated LNCaP tumors showed a significantly greater number of infiltrating CD3+ lymphocytes as compared to DUPA-treated LNCaP tumors (an average 2.5-fold increase). DU145 tumors were not susceptible to treatment, and no significant differences in the number of infiltrating CD3+ lymphocytes were observed in ligand 1- and DUPA-treated DU145 tumors. Staining tumor sections with an anti-CD8 antibody also showed a greater number of infiltrating lymphocytes in LNCaP tumors from the animals treated with conjugate 1 compared to DUPA-treated LNCaP and DU145 tumors (Figure 4f and Supplementary Figure S7h). Immunostaining with an anti-CD4 antibody did not reveal significant differences between tumors obtained from the different experimental groups (Supplementary Figure S7i), suggesting that the population of lymphocytes infiltrating the tumors is largely NK cells and CD8<sup>+</sup> cytotoxic T cells. CD8<sup>+</sup> cytotoxic T lymphocyte (CTL)-dependent immunity is known to contribute to the PBL-dependent suppression of tumor xenografts in hu-PBL-NOD/SCID mouse models.<sup>21–23</sup> The CTL immune response might also be expected to be high in LNCaP tumor cells treated with ligand 1 that are dying by ADCC, since this

mechanism of cytotoxicity can enhance tumor cell immunogenicity.<sup>24</sup> Previous reports suggest that a considerable fraction of the PBL injected into SCID mice might be specific to the host antigens. These observations, taken in conjunction with the high immunogenicity of DU145 cells,<sup>25</sup> can explain a relatively high number of infiltrating CD56<sup>+</sup> and CD3<sup>+</sup> lymphocytes in DU145 tumors, independent of the treatment.

Another reported mechanism of cytotoxic activity associated with therapeutic antibodies is complement-dependent cytotoxicity (CDC), in which antibodies bound to the target tumor fix complement, resulting in formation of the membrane attack complex and cell lysis.<sup>17</sup> Analysis of complement activation in the treated tumors showed increased deposition of C3 complement component in LNCaP tumors exposed to ligand 1 as compared to DUPA-treated LNCaP tumors and DU145 tumors (Supplementary Figure S8). However, because NOD/SCID mice have impaired hemolytic complement activity,<sup>26</sup> CDC cannot be an active mechanism by which ligand 1 reduces growth of LNCaP tumors in the hu-PBL-NOD/SCID mice. Nevertheless, the increased C3 deposition in ligand 1-treated LNCaP suggests that both ADCC and CDC could contribute to anticancer activity of this vaccine in the correct immunological setting as expected for antibody recruitment to the cell surface of target cells.

Further *in vivo* experiments showed that adoptive transfer of mouse anti-DNP serum to SCID mice that lack T cells but retain functional NK cells reduces the size of PSMA-positive LNCaP tumors treated with ligand 1 2.5-fold relative to the mice treated with naive serum and ligand 1 (Figure 5, Supplementary Figure S9). In contrast, PSMA-negative DU145 tumors were not susceptible to ligand 1-mediated cell killing in SCID mice treated with mouse anti-DNP serum, and no significant differences in tumor growth were observed in the treated animal groups. Tumors grown in NSG mice that lack functional T and NK cells were used as the controls and showed no significant differences in tumor growth relative to SCID mice treated with naive serum

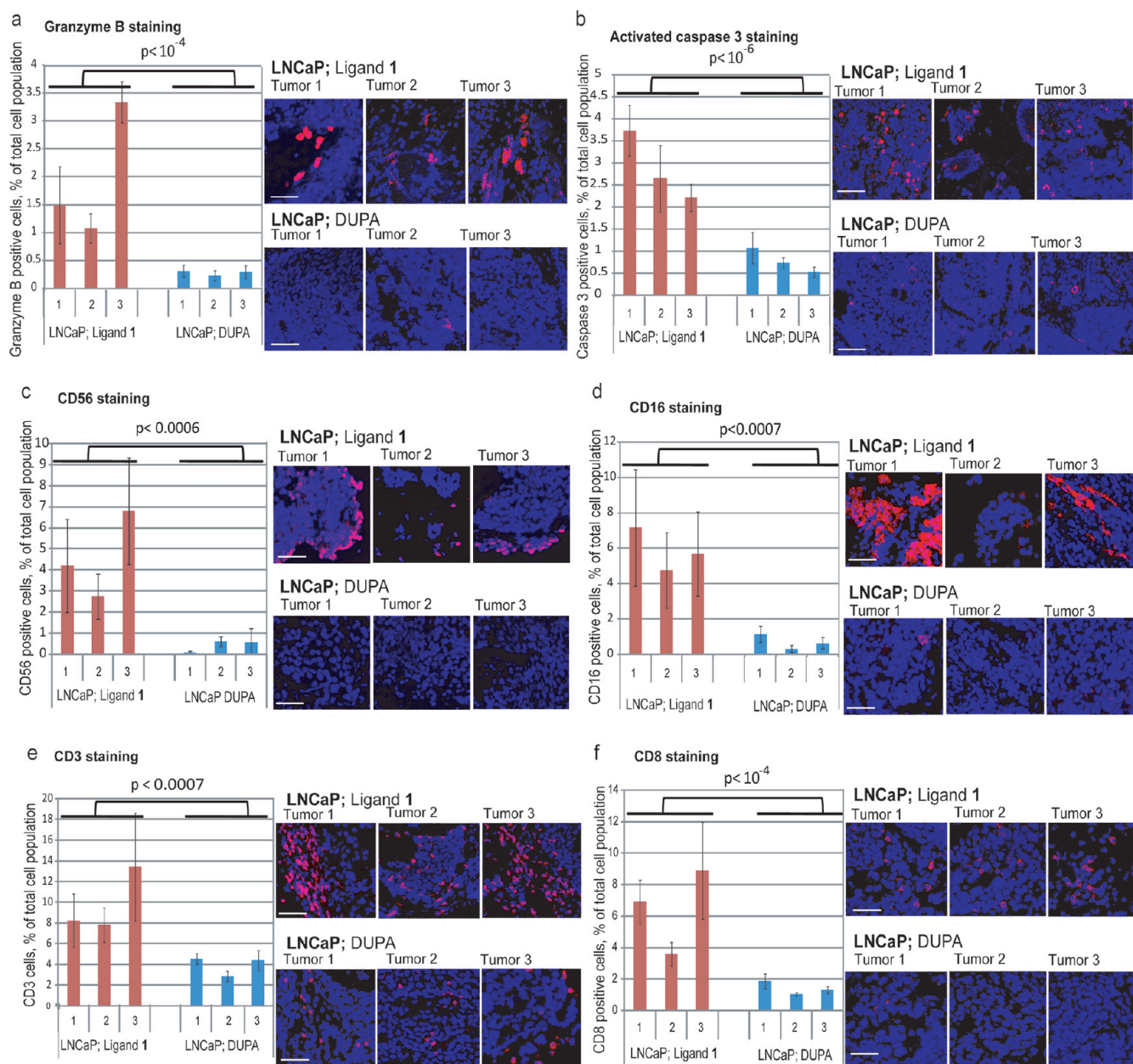


**Figure 4.** Cytotoxic lymphocytes infiltrate ligand 1-treated PSMA-positive tumors. Tumors from ligand 1 and DUPA-treated animals at the conclusion of treatment regimens were harvested, fixed, sectioned, and stained with multiple markers. Immunostaining of the tumor tissue for Granzyme B (a), activated caspase 3 (b), CD56 (c), CD16 (d), CD3 (e), and CD8 (f) revealed enhanced lymphocyte infiltration and cytotoxicity in LNCaP tumors exposed to ligand 1 as compared to DUPA-treated LNCaP tumors and DU145 tumors. Immunostaining procedures were performed at the conclusion of the dosing regimen (6 weeks after mice repopulation with huPBL). Nuclear staining is shown in blue, and granzyme B, activated caspase 3, CD56, CD16, CD3, CD8 staining is shown in red. Cell count and percentage of positive cells are the based on at least 5 fields and >2000 total cells. Error bars represent SEM. Scale bars indicate 100  $\mu\text{m}$ .

and ligand 1 (Figure 5). These results confirm that NK-dependent ADCC is likely an important mechanism mediating ligand 1-dependent cytotoxicity.

PSMA expression is found in other body tissues including the proximal tubules of normal kidney, small bowel, and brain. Biodistribution studies of radioimaging agent DUPA- $^{99\text{m}}\text{Tc}$  showed high uptake of the ligand in kidney (28.9% injected dose per gram of wet tissue) and less than 1% uptake level in the all other normal tissues.<sup>7</sup> However, hematoxylin and eosin (H&E) staining did not reveal morphological changes in spleen and

kidney tissues isolated from hu-PBL-NOD/SCID mice treated with DUPA or ligand 1 (Supplementary Figure S10a). CD8 immunostaining showed no cytotoxic lymphocytes infiltrating into kidney tissues of hu-PBL-NOD/SCID mice treated with ligand 1 (Supplementary Figure S10b). These results indicate that ligand 1-mediated antibody delivery to PSMA-positive cells is not toxic to the other body tissues under this treatment paradigm. Since PSMA expression in normal tissues is on the luminal surface, beyond the epithelial tight junctions, normal cells may be inaccessible to circulating anti-DNP antibodies.<sup>27</sup>

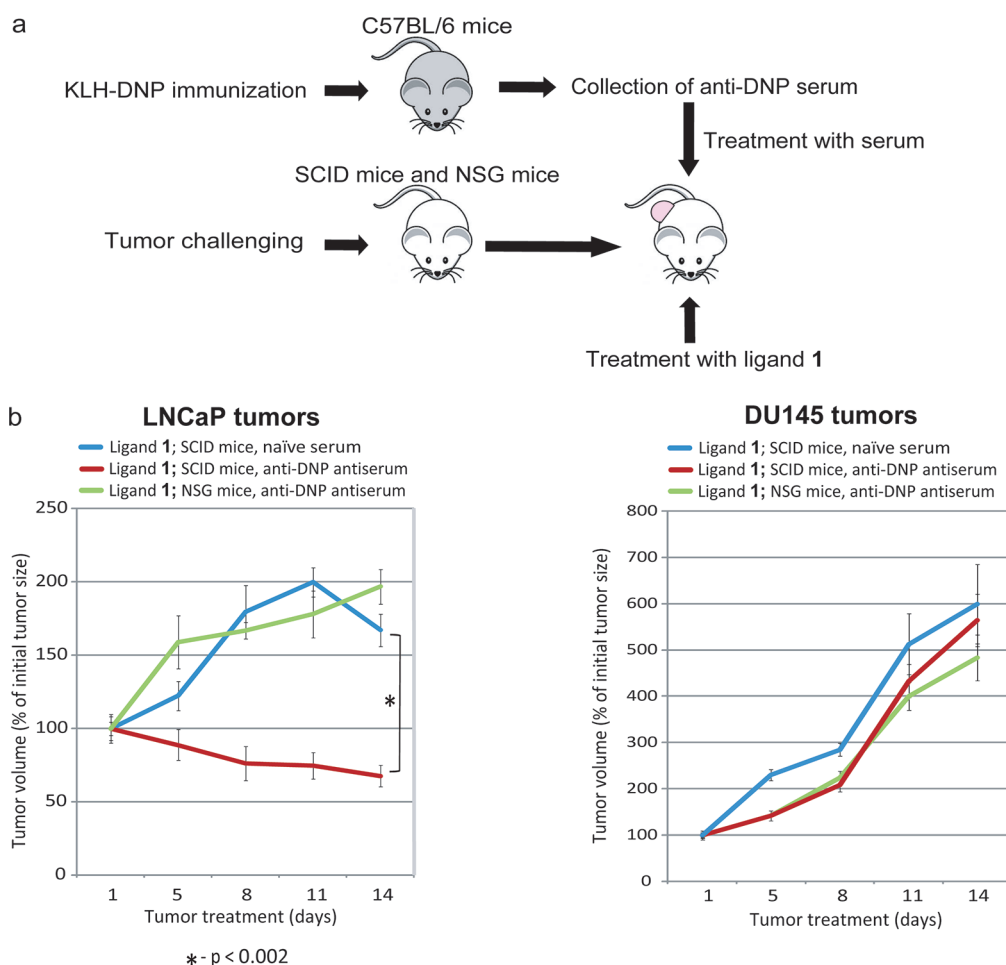


**Figure 5.** NK-dependent ADCC is one of the main mechanisms mediating ligand 1-dependent cytotoxicity. (a) Schematic representation of the experimental plan for the treatment of established tumors. C57BL/6 mice were immunized with DNP-KLH ( $100 \mu\text{g}$  of DNP-KLH in PBS emulsified 1:1 with complete Freund's Adjuvant). A second immunization with DNP-KLH was performed 2 weeks after the first ( $100 \mu\text{g}$  of DNP-KLH in PBS emulsified 1:1 with incomplete Freund's Adjuvant), and the serum was collected 2 weeks after.  $5 \times 10^5$  LNCaP and  $5 \times 10^4$  DU145 cells were injected sc into SCID and NSG mice and formed xenograft tumors for 10 days. SCID mice and NSG mice bearing xenograft human tumors were treated with ligand 1 in PBS ( $4 \text{ mg/kg}$ , iv) and with mouse anti-DNP or naïve serum ( $50 \mu\text{L}$ , ip) three times per week for 2 weeks. Tumor measurements were taken every 3–4 days. (b) The adoptive transfer of mouse anti-DNP serum to SCID mice that lack T cells but retain functional NK cells reduces the size of PSMA-positive tumors treated with ligand 1 2.5-fold relative to the control groups treated with naïve serum. In contrast, PSMA-negative tumors were not susceptible to ligand 1-mediated cell killing, and no significant differences in tumor growth were observed in the treated animal groups. Tumors grown in NSG mice that lack functional T and NK cells were used as the controls and showed no significant differences in tumor growth relative to SCID mice treated with naïve serum and ligand 1. Each experimental group contained at least five mice. Error bars represent SEM.

In conclusion, we have established an *in vivo* model for a drug-inducible therapeutic anticancer vaccine and reported the efficacy of the vaccine against PSMA-positive prostate cancer xenografts. The strategies that have been reported<sup>7,8</sup> require preimmunization with a hapten-carrier conjugate to generate the antibodies that mediate ligand-induced ADCC, whereas our approach utilizes endogenous antibodies and thus no such preparation is needed. The advantage of our strategy compared with other cancer vaccines comes from the fact that the DNP group is able to recruit endogenous anti-DNP antibodies to target PSMA-positive prostate tumors and elicit an antitumor response. Our observations and previous reports suggest that anti-DNP antibodies are abundant in the human bloodstream and competent to mediate targeted cytotoxicity that makes them a powerful tool for development of a drug-inducible therapeutic vaccine. Indeed, the titer of anti-DNP antibodies in the serum of immunized mice used in our model is comparable to the level

found in normal human blood. In addition, in contrast to previous reports our study used a humanized immune system and xenografts of well-studied human prostate cancer cells, underscoring our use of a highly cancer-specific small molecule for the recruitment of endogenous antibodies.

The utility of this approach relative to more conventional vaccines is that one "universal antigen" can be used to generate a non-self immune response that can then be directed to the desired target cells by exposure to an appropriate bifunctional adapter molecule (e.g., prostate cancer with PSMA-specific ligand or breast cancer with CXCR4-specific ligand). Moreover, it should be possible to also deliver a therapeutic immune response to pathogens using conserved ligand binding sites such as the active binding site of influenza neuraminidase. This strategy has the potential to combine the power of classical anticancer vaccines with the attractive pharmacological properties of small molecules and thus opens new therapeutic options to fight disease.

## METHODS

**Cells and Animals.** DU145 and LNCaP (prostate cancer cells) were obtained from ATCC and cultured in Dulbecco's Minimal Essential Medium (DU145 cells) or RPMI-1640 Medium (LNCaP cells), supplemented with 10% fetal calf serum, 300  $\mu\text{g}/\text{mL}$  of glutamine, 100 IU/mL of penicillin and 100  $\mu\text{g}/\text{mL}$  of streptomycin. NOD.CB17-Prkdc (SCID) mice obtained from Jackson Laboratories were used at 4 weeks of age and maintained under standard conditions according to institutional guidelines.

**Mouse Engraftment and Treatment.** Human peripheral blood mononuclear cells (PBMC) were obtained from the peripheral blood of healthy donors. All donors were screened for HIV type 1 (HIV-1) and hepatitis prior to donation. PBMC were purified following conventional procedures (enriched by Ficoll-Hypaque gradient centrifugation). RBC Lysis Solution (Qiagen) was used to lyse red blood cells. Twenty million cells were resuspended in 0.3 mL of PBS and injected ip into the recipient mice. Fourteen days after lymphocyte reconstruction, mice were immunized ip with 200  $\mu\text{L}$  of DNP-KLH at a concentration of 1 mg/mL emulsified with complete Freund's Adjuvant (adjuvant: antigen emulsified mixture of 1:1). Mice were boosted 14 days after the first immunization with the same dose of DNP-KLH at a concentration of 1 mg/mL emulsified with incomplete Freund's Adjuvant (adjuvant/antigen emulsified mixture of 1:1). The mice were bled every 2 weeks after repopulation. The tumor treatment experiment was performed according to the scheme in Supplementary Figure S5. Three days after the first immunization,  $5 \times 10^5$  LNCaP cells or  $5 \times 10^4$  DU145 cells were injected sc in 100  $\mu\text{L}$  of BD matrigel (BD Biosciences) into the right flank of mice. Following the tumor cell challenge, tumor development and mice weights were monitored twice weekly. Two weeks after the tumor challenge, when the tumors reached a size of 50–70  $\text{mm}^3$ , mice were treated with DUPA (4 mg/kg, iv) or ligand 1 (4 mg/kg, iv) three times per week for 2 weeks. Each experimental group contained at least five mice. The tumors were measured every 4–5 days. After treatment was terminated, mouse body weight was  $\pm 15\%$  of the initial weight (Supplementary Figure S10). Control experiments were performed with NOD.CB17-Prkdc (SCID) mice that were not engrafted with human PBMC. Control experiments were performed in the same conditions as for hu-PBL-NOD/SCID mice. *In vivo* experiments were performed twice to ensure reproducibility. For the adoptive serum transfer experiment, C57BL/6 mice were immunized with DNP-KLH (100  $\mu\text{g}$  of DNP-KLH in PBS emulsified 1:1 with complete Freund's Adjuvant). A second immunization with DNP-KLH was performed 2 weeks after the first (100  $\mu\text{g}$  of DNP-KLH in PBS emulsified 1:1 with incomplete Freund's Adjuvant), and the serum was collected 2 weeks after. Five  $\times 10^5$  LNCaP and  $5 \times 10^4$  DU145 cells were injected sc into SCID and NSG mice and formed xenograft tumors for 10 days. SCID mice and NSG mice bearing xenograft human tumors were treated with ligand 1 in PBS (4 mg/kg, iv) and with mouse anti-DNP or naive serum (50  $\mu\text{L}$ , ip) three times per week for 2 weeks. Tumor measurements were taken every 3–4 days. All the mice were housed according to national and institutional guidelines for humane animal care.

**ADCC Assays.** LNCaP and DU145 cells were briefly dissociated with 0.05% trypsin/EDTA solution (HyClone) and washed twice in ADCC medium (RPMI supplemented with 1% fetal calf serum). Cells were incubated with Calcein-AM (5  $\mu\text{M}$  solution in ADCC medium) for 1 h at 37  $^\circ\text{C}$ , 5%  $\text{CO}_2$ , washed twice with ADCC medium, adjusted to concentration  $2.5 \times 10^5$  cells/mL, and plated onto clear flat-bottom 96-well plates at  $1.25 \times 10^4$  cells/well (50  $\mu\text{L}$  per well). Separately, PBMC were prepared following conventional procedures (enriched by Ficoll-Hypaque gradient centrifugation). RBC Lysis Solution (Qiagen) was used to lyse red blood cells. PBMC were washed and resuspended in ADCC medium. Anti-DNP antiserum at various concentrations (3.5–20  $\mu\text{g}/\text{mL}$ , as measured relative to commercial anti-DNP antibody, Invitrogen), ligand

1 (62 nM), and DUPA (100 nM) were added to the wells and plates were incubated at 37  $^\circ\text{C}$ , 5%  $\text{CO}_2$  for 60 min. Pooled anti-DNP serum from 3 mice was used for each experiment. Following the incubation period, human PBMC (20:1 effector/target ratio) were added. Target cell maximum killing was achieved by adding Triton X-100 to the cell suspension to a final concentration 1%. Control experiments to determine spontaneous cytotoxicity due to nonspecific killing were performed using LNCaP cells, effector cells, ligand 1, and antiserum from nonimmunized hu-PBL-NOD/SCID mice. After incubation at 37  $^\circ\text{C}$ , 5%  $\text{CO}_2$  for 4 h, sample fluorescence was analyzed using an Acquest spectrofluorimeter (excitation at 485 nm, emission at 530 nm). Control experiments were performed using PSMA-negative DU145 cells. Percent cytotoxicity was calculated using the following formula:

$$\% \text{Cytotoxicity} = \frac{(\text{Fluorescence expt} - \text{Fluorescence spontaneous average})}{(\text{Fluorescence max killing average} - \text{Fluorescence spontaneous average})} \times 100\%$$

**Flow Cytometry Analysis.** LNCaP and DU145 cells were dissociated with Accutase (Innovative Cell Tech Inc.) and washed twice in staining solution containing  $\text{Ca}^{2+}$ - and  $\text{Mg}^{2+}$ -free PBS with 1 mM ethylenediaminetetraacetic acid (EDTA), 25 mM HEPES (pH 7.0) (Invitrogen), and 0.5% FBS. Mouse serum from nonimmunized hu-PBL-NOD/SCID mice was added to final concentration of 10% to LNCaP and DU-145 cell suspensions, and cells were then incubated at RT for 30 min. The cells were cooled on ice, one part of each suspension was transferred to new Eppendorf tubes, a solution of DUPA in PBS was added to a final concentration of 100 nM, and cells were then incubated for 30 min. DUPA-treated and untreated cell suspensions were incubated with ligand 1 (62 nM) followed by anti-DNP antiserum at a dilution of 1:5 and APC conjugated goat antihuman IgG (Jackson ImmunoResearch Laboratories) at a dilution of 1:200. Experiments were protected from light and incubated on ice for 30 min. Mouse serum from nonimmunized hu-PBL-NOD/SCID mice was used as an IgG control. Alternatively, flow cytometry experiments were performed using Alexa Fluor 488 conjugated rabbit antidinitrophenyl IgG (Invitrogen). Ligand 1 (200 nM) or DUPA (5  $\mu\text{M}$ ) plus ligand 1 (200 nM) (competition experiment) were added to cells followed by Alexa Fluor 488 conjugated rabbit antidinitrophenyl IgG (Invitrogen) at a concentration of 10  $\mu\text{g}/\text{mL}$ . Samples were analyzed on a BD LSR II flow cytometer (Beckton Dickinson Immunocytometry Systems). Cell debris and clumps were electronically gated. A minimum of 500,000 viable cell events were collected per sample. The data was analyzed using FlowJo software (Tree Star Inc.). To analyze the total splenocyte population for the presence of CD4+ human lymphocytes, the spleens were isolated from hu-PBL-NOD/SCID mice and control NOD/SCID mice on day 45 after lymphocyte reconstruction. Tissues were cut into small pieces of approximately 5 mm and transferred to a 10 cm tissue dish containing 5 mL of serum-free Medium 199. Tissues were digested with 225 U/mL collagenase 3 (Collagenase Type3, Worthington 56E8800) at 37  $^\circ\text{C}$ , 5%  $\text{CO}_2$  for 2–3 h depending on the tumor size. The dissociated tissues were filtered twice using 100 and 40  $\mu\text{m}$  cell strainers (BD Falcon). RBC Lysis Solution (Qiagen) was used to lyse red blood cells. The cell suspension was washed twice in staining solution and stained with conjugated anti-CD4 (mouse antihuman CD4-APC, Miltenyi Biotec) antibody at a dilution of 1:11 (50 min at 4  $^\circ\text{C}$ ). Samples were analyzed on a BD LSR II flow cytometer (Beckton Dickinson Immunocytometry Systems). Cell debris and clumps were electronically gated. A minimum of 500,000 viable cell events were collected per sample. The data was analyzed using FlowJo software (Tree Star Inc.).

**Histology and Immunofluorescence.** For cryosectioning, the tumor, spleen, and kidney tissues isolated from animals of each experimental group were fixed by immersion in 4% paraformaldehyde, cryoprotected in 20% sucrose, frozen, and embedded in sucrose/OCT

(1:1). Cryostat sections (12  $\mu\text{m}$ ) were collected on Superfrost plus slides and subjected to routine hematoxylin/eosin (H&E) and immunofluorescent staining. For immunostaining, slides were preincubated 30 min in antibody buffer (50 mM NaCl, 50 mM Tris Base, 1% BSA, 100 mM L-lysine, 0.04% sodium azide [pH 7.4]) containing 0.4% Triton and 10% serum and then incubated overnight at 4 °C with the primary antibodies CD56 (BioLegend, 304602, dilution 1:50), CD16 (BD Pharmingen, 550383; dilution 1:50), CD8 (Spring Bioscience, dilution 1:200), Granzyme B (Abcam, ab4059; dilution 1:100), Caspase 3 (Cell Signaling Technology, 9664; dilution 1:200) or C3 (Santa Cruz Biotechnology, Inc., V-20; dilution 1:100). Bound antibodies were detected with appropriate secondary antibodies conjugated with Alexa 488 or 555 (Invitrogen, dilution 1:1000) diluted in antibody buffer at RT for 1 h. The anti-CD16 antibody was visualized by a three-step staining procedure in combination with biotin-conjugated antimouse Igs (Invitrogen) as the secondary antibody and streptavidin, Alexa Fluor 555 conjugate (Invitrogen). The slides were mounted with the Mowiol mounting medium (9.6% Mowiol, 24% glycerol, 0.1 M Tris HCL [pH 7.4]) containing 1  $\mu\text{M}$  Hoechst 33342 (Invitrogen). TUNEL assay was performed using The DeadEnd Fluorometric TUNEL System (Promega) accordingly to manufacturer's recommendations. Tissue staining was analyzed using an UltraVIEW VoX confocal microscope (PerkinElmer). For quantification, cells in at least five randomly selected fields of view were counted for each condition. Control experiments were performed with tumor, spleen, and kidney tissues isolated from NOD/SCID mice that were not engrafted with human PBMC. Control experiments were performed under the same conditions as for the tissues isolated from hu-PBL-NOD/SCID mice. Each staining was performed for three tumor samples from two independent *in vivo* experiments to ensure reproducibility.

**ELISA for Human and Mouse Anti-DNP IgG.** Analysis of anti-DNP IgG in mouse serum was performed by enzyme-linked immunosorbent assay (ELISA). ELISA Starter Accessory Kit was purchased from Bethyl Laboratories. Assays were performed according to manufacturer's recommendation. Briefly, the high-binding 96-well plates (Costar, Cambridge, MA) were coated with DNP-bovine serum albumin (BSA) conjugate at concentration 1  $\mu\text{g}/\text{mL}$ , and remaining binding sites were blocked with 1% BSA in PBS for 12 h at 4 °C. BSA-coated wells served as a negative control, and noncoated wells served as a blank control. The mouse serum was collected by retro-orbital bleeds 2 weeks after second immunization. Human and mouse sera were serially diluted using blocking solution, 100  $\mu\text{L}$  of diluted sera was added to each well, and the plate was incubated for 1 h at RT. The plate was washed with PBS, 100  $\mu\text{L}$  of HRP-conjugated goat antihuman IgG (Santa Cruz Biotechnology, Inc.) or HRP-conjugated goat antimouse IgG/IgM/IgA (Thermo Scientific) diluted 1:700 or 1:1000, respectively, in blocking buffer was added to each well, and the plate was incubated for 1 h at RT. Plates were analyzed using a SpectraMax Plus384 Absorbance Microplate Reader (Molecular Devices).

**Fluorescent Microscopy Experiment.** LNCaP cells were plated in a 384-well black clear bottom plate (Greiner Bio-One) at a density of 1000 cells per well in medium containing 10% serum. Cells were grown until they reached 40–60% confluence (approximately 3–4 days), 100% horse serum was added to each well to block Fc receptors, and cultures were incubated at RT for 15 min. Ligand 1 (62 nM) and DUPA (100 nM) were added into the wells in RPMI medium containing 1% fetal calf serum followed by mouse anti-DNP antiserum at a dilution of 1:11 and R-PE conjugated goat antihuman Ig (IgM+IgG+IgA, H+L) at a dilution of 1:100. The serum from nonimmunized hu-PBL-NOD/SCID mice was used for negative control experiments was added. Cultures were protected from light and incubated at 37 °C for 60 min. The wells were washed with PBS, fixed by addition of 100  $\mu\text{L}$  of paraformaldehyde (3.7% in PBS), and incubated at 37 °C for 30 min. Wells were washed with PBS (10  $\times$  100  $\mu\text{m}$ ). Cells were analyzed using an UltraVIEW VoX confocal microscope (PerkinElmer).

**BIND Assay.** SRU 384-well GA3 plates were allowed to warm to 25 °C, and were washed 5 times with assay buffer (100 mM HEPES, 50 mM KCl, 0.5 mM MgCl<sub>2</sub>, pH 7.5) to remove glycerol. Each well was equilibrated with 25  $\mu\text{L}$  of assay buffer; this volume was kept consistent through subsequent steps. Equilibration reads were performed on a SRU Profiler BIND Reader. After signal stabilization, the wells were aspirated of assay buffer, and 30  $\mu\text{g}/\text{mL}$  of anti-DNP antibody (clone SPE-7, Sigma Aldrich) in assay buffer was added to each well and allowed to incubate for 3 h. Sensor plates were read to confirm the PWV shift, then washed 3 times with assay buffer to remove residual antibody, and read again. Then 100 nM PSMA and 300 nM DUPA or ligand 1 was added to the corresponding wells for 3 h and read again to record the final result.

**Statistical Analysis.** The results of histological analysis, flow cytometry assays and *in vivo* tumorigenicity assays were analyzed by paired *t* test. A *p* value of <0.05 was regarded as statistically significant.

## ■ ASSOCIATED CONTENT

**S Supporting Information.** Supplementary figures and extended experimental procedures. This material is available free of charge via the Internet at <http://pubs.acs.org>.

## ■ AUTHOR INFORMATION

### Corresponding Author

\*E-mail: [schultz@scripps.edu](mailto:schultz@scripps.edu); [ccho@gfnf.org](mailto:ccho@gfnf.org).

### Author Contributions

<sup>†</sup>These authors contributed equally to this work.

## ■ ACKNOWLEDGMENT

We thank C. Schmedt and I. Engels for helpful discussions and S. Espinosa for technical assistance. This study was supported by Susan G. Komen for the Cure Grant PDF0707903 (to A.D.). This work was supported by the Novartis Research Foundation and The Skaggs Institute for Chemical Biology.

## ■ REFERENCES

- (1) Olson, W. C., Heston, W. D., and Rajasekaran, A. K. (2007) Clinical trials of cancer therapies targeting prostate-specific membrane antigen. *Rev. Recent Clin. Trials* 2, 182–190.
- (2) Higano, C. S., Small, E. J., Schellhammer, P., Yasothan, U., Gubernick, S., Kirkpatrick, P., and Kantoff, P. W. (2010) Sipuleucel-T. *Nat. Rev. Drug Discovery* 9, 513–514.
- (3) Bodey, B., Bodey, B., Jr, Siegel, S. E., and Kaiser, H. E. (2000) Failure of cancer vaccines: the significant limitations of this approach to immunotherapy. *Anticancer Res.* 21, 2665–2676.
- (4) Costello, R. T., Gastaut, J. A., and Olive, D. (1999) Tumor escape from immune surveillance. *Arch. Immunol. Ther. Exp.* 47, 83–88.
- (5) Doehn, C., Böhmer, T., Kausch, I., Sommerauer, M., and Jocham, D. (2008) Prostate cancer vaccines: current status and future potential. *Biodrugs* 22, 71–84.
- (6) Shokat, K. M., and Schultz, P. G. (1991) Redirecting the immune response: Ligand-mediated immunogenicity. *J. Am. Chem. Soc.* 113, 1861–1862.
- (7) Popkov, M., Gonzalez, B., Sinha, S. C., and Barbas, C. F. (2009) Instant immunity through chemically programmable vaccination and covalent self-assembly. *Proc. Natl. Acad. Sci. U.S.A.* 106, 4378–4383.
- (8) Lu, Y., and Low, P. S. (2002) Folate targeting of haptens to cancer cell surfaces mediates immunotherapy of syngeneic murine tumors. *Cancer Immunol. Immunother.* 51, 153–162.
- (9) Elsasser-Beile, U., Buhler, P., and Wolf, P. (2009) Targeted therapies for prostate cancer against the prostate specific membrane antigen. *Curr. Drug Targets* 8, 118–125.



- (10) Kozikowski, A. P., Zhang, J., Nan, F., Petukhov, P. A., Grajkowska, E., Wroblewski, J. T., Yamamoto, T., Bzdega, T., Wroblewska, B., and Neale, J. H. (2004) Synthesis of urea-based inhibitors as active site probes of glutamate carboxypeptidase II: efficacy as analgesic agents. *J. Med. Chem.* *47*, 1729–1738.
- (11) Kularatne, S. A., Wang, K., Santhapuram, H. K., and Low, P. S. (2009) Prostate-specific membrane antigen targeted imaging and therapy of prostate cancer using a PSMA inhibitor as a homing ligand. *Mol. Pharmaceutics* *6*, 780–789.
- (12) Murelli, R. P., Zhang, A. X., Michel, J., Jorgensen, W. L., and Spiegel, D. A. (2009) Chemical control over immune recognition: a class of antibody-recruiting small molecules that target prostate cancer. *J. Am. Chem. Soc.* *131*, 17090–17092.
- (13) Tary-Lehmann, M., Saxon, A., and Lehmann, P. V. (1995) The human immune system in hu-PBL-SCID mice. *Immunol. Today* *16*, 529–533.
- (14) Farah, F. S. (1973) Natural antibodies specific to the 2, 4-dinitrophenyl group. *Immunology* *25*, 217–226.
- (15) Muller-Eberhard, H. J. (1998) Molecular organization and function of the complement system. *Annu. Rev. Biochem.* *57*, 321–347.
- (16) Sun, P. D. (2003) Structure and function of natural-killer-cell receptors. *Immunol. Res.* *27*, 539–548.
- (17) Clynes, R. A., Towers, T. L., Presta, L. G., and Ravetch, J. V. (2000) Inhibitory Fc receptors modulate in vivo cytotoxicity against tumor targets. *Nat. Med.* *6*, 443–446.
- (18) Natsume, A., Niwa, R., and Satoh, M. (2009) Improving effector functions of antibodies for cancer treatment: Enhancing ADCC and CDC. *Drug Des., Dev. Ther.* *21*, 7–16.
- (19) Afonina, I. S., Cullen, S. P., and Martin, S. J. (2010) Cytotoxic and non-cytotoxic roles of the CTL/NK protease granzyme B. *Immunol. Rev.* *235*, 105–116.
- (20) Julius, M., Maroun, C. R., and Haughn, L. (1993) Distinct roles for CD4 and CD8 as co-receptors in antigen receptor signaling. *Immunol. Today* *14*, 177–183.
- (21) Iwanuma, Y., Chen, F. A., Egilmez, N. K., Takita, H., and Bankert, R. B. (1997) Antitumor immune response of human peripheral blood lymphocytes coengrafted with tumor into severe combined immunodeficient mice. *Cancer Res.* *57*, 2937–2942.
- (22) Toes, R. E., Blom, R. J., van der Voort, E., Offringa, R., Melief, C. J., and Kast, W. M. (1996) Protective antitumor immunity induced by immunization with completely allogeneic tumor cells. *Cancer Res.* *56*, 3782–3787.
- (23) Hölscher, C., Hasch, G., Joswig, N., Stauffer, U., Müller, U., and Mossmann, H. (1999) Long term substitution and specific immune responses after transfer of bovine peripheral blood lymphocytes into severe combined immunodeficient mice. *Vet. Immunol. Immunopathol.* *70*, 67–83.
- (24) Dhodapkar, M., Dhodapkar, K., and Li, Z. (2008) Role of chaperone and Fc $\gamma$ R in immunogenic death. *Curr. Opinion in Immunology* *20*, 512–517.
- (25) Popkov, M., Rader, C., and Barbas, C. F., III (2004) Isolation of human prostate cancer cell reactive antibodies using phage display technology. *J. Immunol. Methods* *291*, 137–151.
- (26) Shultz, L. D., Schweitzer, P. A., Christianson, S. W., Gott, B., Schweitzer, I. B., Tennent, B., McKenna, S., Mobraaten, L., Rajan, T. V., and Greiner, D. L. (1995) Multiple defects in innate and adaptive immunologic function in NOD/LtSz-scid mice. *J. Immunol.* *54*, 180–191.
- (27) Milowsky, M. I., Nanus, D. M., Kostakoglu, L., Sheehan, C. E., Vallabhajosula, S., Goldsmith, S. J., Ross, J. S., and Bander, N. H. (2007) Vascular targeted therapy with anti-prostate-specific membrane antigen monoclonal antibody J591 in advanced solid tumors. *J. Clin. Oncol.* *25*, 540–547.